ELSEVIER

Journal of Nuclear Materials 270 (1999) 147–153

journal of nuclear materials

Kinetic studies on massive hydriding of commercial zirconium alloy tubing

Yong-soo Kim *, Sun-ki Kim

Department of Nuclear Engineering, Hanyang University, 17 Haengdang-Dong, Sungdong-Ku, Seoul 133-791, South Korea

Received 7 May 1998; accepted 19 October 1998

Abstract

Kinetic studies on the massive hydriding of commercial Zircaloy-2, Zircaloy-4, and ZIRLO™ tubes are carried out in the temperature range 300–500°C under atmospheric pressure by in situ measurements with TGA (thermo-gravimetric apparatus). The results show that hydriding kinetics follows a linear rate law after incubation time caused by the thin surface oxide film grown during inevitable prior heating. The reaction rate constants derived on the basis of the linear kinetics are $1.1 \times 10^7 \exp(-87.0/RT)$, $6.9 \times 10^7 \exp(-100/RT)$, and $1.5 \times 10^6 \exp(-75.3/RT)$ mg/dm^2 min for Zircaloy-2, Zircaloy-4, and ZIRLO™, respectively, where the activation energy is in kJ/mol. Slight retardations from the linear kinetic behaviors are observed at temperatures lower than 400°C. It is attributed to slow diffusion of hydrogen atoms through hydride layer at the low temperatures. Despite the lack of temperature gradient, sunburst-type localized massive hydridings are unexpectedly observed mostly at the inner surfaces of specimens, even with hydrogen content of around 1000 ppm. This demonstrates the importance of surface condition in the massive hydriding of zirconium alloy tubes.

1. Introduction

Under in-reactor operating conditions, Zircaloy fuel cladding can be exposed to through-wall defects resulting from debris damage or fretting, corrosion, PCI (pellet cladding interaction), etc. Once the through-wall defect forms, coolant water enters the gap between the pellet and the clad through the defect hole since the coolant pressure is much greater than the internal fuel rod pressure. Then, the coolant flashes into steam in the gap, and after a few hours or days later, pressure equalization between the gap plenum and the coolant is achieved. Next, the following processes take place in the gap: oxidation of inner surface of Zircaloy clad, radiolytic decomposition of steam by fission fragments, and fuel oxidation by steam. As a result of these processes, steam concentration decreases with time and hydrogen concentration builds up continuously as a reaction product. When the oxide film grown by the steam oxidation remains protective, only the regular hydrogen pick-up by the Zircaloy base metal takes place, and thus, massive hydriding and its resultant catastrophic cladding failure cannot occur. However, if the ratio of hydrogen to steam pressure exceeds a critical value, the protective property of the oxide is suddenly lost and massive hydrogen absorption can take place rapidly. This phenomenon is called 'secondary hydriding' of fuel cladding.

In actuality, this massive hydriding, primary or secondary, is regarded as one of the potential causes of fuel failures under high burn-up and extended fuel cycle operation. The critical ratio is known to be order of 10^2–10^6 depending on temperature, pressure, surface condition, and oxide property [1–3]. A schematic illustration of the secondary hydriding process in a defective fuel rod is given in Fig. 1.

Until now, however, only a few papers have been published on the kinetics and conditions of the massive hydriding of Zircaloys, and thus, they are not clearly established. Early researchers reported that the kinetics follows a parabolic rate law associated with the hydrogen diffusion process [4,5]. On the other hand, some

* Corresponding author. Tel.: +82-22 290 0467; fax: +82-22 281 5131; e-mail. yongskim@numater.hanyang.ac.kr

0022-3115/99/$ – see front matter
PII: S0022-3115(98)00902-7

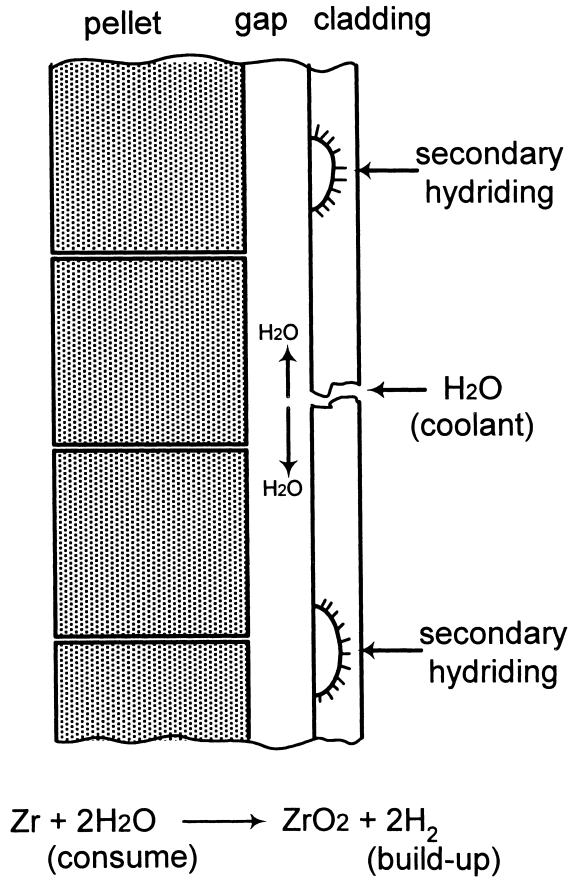

Fig. 1. A schematic illustration of hydriding process of the cladding in a defective fuel rod.

workers later in around 1980 claimed it is controlled by surface-reaction, i.e., follows a linear rate law [6,7]. However, since then, no detailed kinetic data such as activation energy and pre-exponential factor have been reported except for the hydriding of Zircaloy-2 tube [6].

Therefore, the purpose of the present investigation is to bring the basics of Zircaloy massive hydriding into the current secondary hydriding issues and to provide kinetic data on the hydriding of commercial zirconium alloy tubing.

2. Experimental

TGA (thermo-gravimetric apparatus) experiments under atmospheric pressure are carried out in the temperature range of 300–500°C to measure the weight gain due to hydrogen absorption. A schematic diagram of the apparatus is shown in Fig. 2. The specimen is suspended by a platinum wire connected to a quartz beam in the micro-balance weighing cell which is maintained at room temperature by circulating coolant water (Fig. 2). The weighing cell and the whole reaction chamber are covered with helium gas prior to the actual experiments to prevent the specimens from oxidation during heating to reaction temperature. When the temperature of the reaction chamber reaches the desired temperature, the flow of hydrogen gas into the reaction chamber is initiated at the flow rate of 200 cc/min. The sensitivity of the electro-micro-balance system (model S3D-P, Satorius) is 1 μg.

Samples used in the experiments are Sandvik Zircaloy-2, low-tin Zircaloy-4, and Westinghouse ZIRLO™ tubes. They are cut in 1 cm length (equivalent to ~1.1 g) with a diamond-wafered low speed saw, pickled in a solution of 50% H_2O + 47% HNO_3 + 3% HF for 3 min to remove pre-filmed surface oxide, and cleaned in acetone ultrasonically.

The weight gain is continuously measured in a time interval ranging from 6 s to 3 min and the data is acquired by a data acquisition system connected to a personal computer. The experiment is completed by sudden weight gain decrease caused by flaking-off of the embrittled specimen. Both the hydrogen and helium gas purities are 99.999%.

3. Results and discussion

First, weight gain behaviors of Zircaloy-2, Zircaloy-4, and ZIRLO™ tubes are compared and plotted at two temperatures, 300°C and 400°C, in Fig. 3. As seen in the figure, little weight gain by the hydrogen absorption is observed at the initial stage for a certain period of time, but after the incubation period, weight gain increases rapidly, almost linearly with reaction time.

At 300°C, the incubation time of Zircaloy-4 tube is the longest (about 30 h) while those of the Zircaloy-2 and ZIRLO™ tubes are similar (~1000 and ~800 min, respectively). However, at 400°C, the incubation periods become very short and almost identical, regardless of the kinds of zirconium alloy tubes. The figure also shows that the weight gain rates of the zirconium alloy tubes at the two temperatures are not much different, and if arranged, they are in the order of ZIRLO™ > Zircaloy-2 > Zircaloy-4. In fact, it is well-known that the rate of weight gain is irrelevant to incubation time.

It is also well-known that surface oxide film prevents hydrogen from being absorbed by Zircaloy base metal and the incubation time is basically proportional to the oxide thickness as long as the film is protective [6]. Several techniques have been tried to avoid surface oxidation; however, it was recently reported that the surface oxide film always forms during prior heating of the chamber even under a vacuum of 10^{-7} Torr, and thus, surface oxidation is inevitable [8,9]. As expected, SEM/EDX (scanning electron microscope/energy dispersive

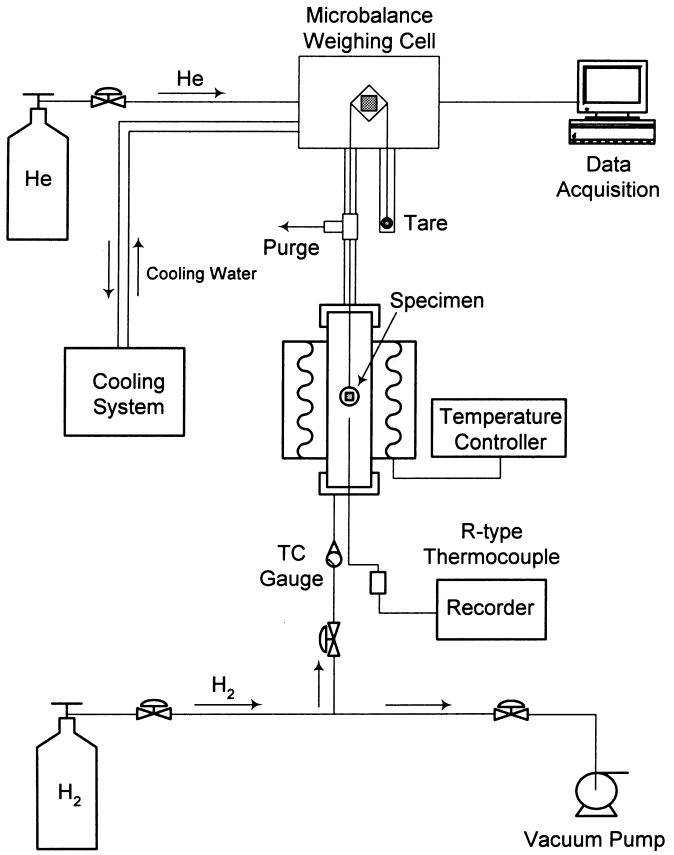

Fig. 2. A schematic diagram of TGA.

X-ray spectrometer) analysis shows the oxygen concentration profiles in the cross-sectioned hydrided zirconium alloy tubes, confirming that the incubation times in the current investigation are also attributed to thin surface oxide film formed even in the inert helium environment during the prior heating (Fig. 4).

Once the incubation terminates, the weight gain resulting from hydrogen absorption increases rapidly with time. First, the morphologies of hydrided zirconium alloy tubes are examined to estimate hydride distribution and orientation. Those of the three commercial zirconium alloy tubes hydrided around 5000 ppm are shown in Fig. 5. In fact, 1 mg of weight gain in this study is equivalent to hydrogen content of about 900 ppm. In the cases of the Zircaloy-2 and -4 tubes, hydride distributions and orientations are similarly random. On the other hand, radial hydrides are clearly observed in the case of the ZIRLO™ tube. In all cases, the edges of the specimens are not extraordinarily hydrided and repeated examinations demonstrate that these morphologies are typically observed.

For detailed kinetics studies, the weight gain behaviors of Zircaloy-2, Zircaloy-4, and ZIRLO™ tubes are investigated in the temperature range of 300–500°C (Fig. 6(a)–(c)). All figures reveal that the incubation time is not observed at temperatures higher than 400°C, and once the massive hydrogen absorption is initiated, the weight gain rapidly increases in proportion to the reaction time. This means that the hydriding kinetics follows a linear rate law, which indicates that the reaction is not diffusion-controlled but surface-reaction controlled.

Therefore, weight gain rate can be expressed as follows:

$$\Delta W = kt, \tag{1}$$

where ΔW is weight gain in mg/dm^2, t is reaction time in minutes, and k is the reaction rate constant in mg/dm^2 min. In fact, the rate constant k consists of two terms, pre-exponential factor k_0 and activation energy Q as shown:

$$k = k_0 \exp\left(-\frac{Q}{RT}\right), \tag{2}$$

where R is the gas constant and T is absolute temperature in Kelvin. On the basis of the linear rate law, the kinetic

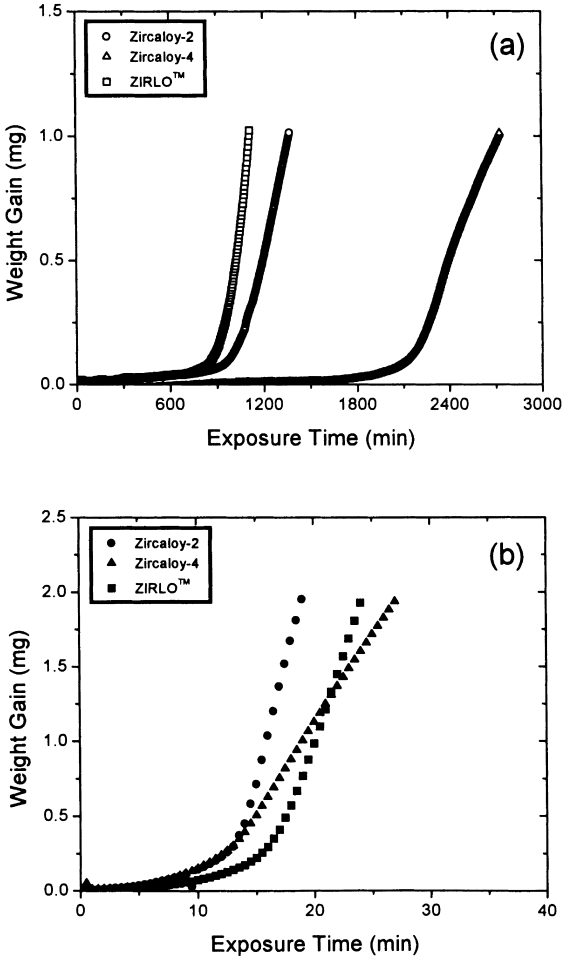

Fig. 3. Comparison of weight gains of Zircaloy-2, Zircaloy-4, and ZIRLO™ tubes with reaction time: (a) at 300°C and (b) at 400°C.

constants are derived by using Arrhenius plots of weight gain rates from the previous three figures for Zircaloy-2, Zircaloy-4, and ZIRLO™ tubes (Fig. 7(a)–(c)).

The reaction rate constants consisting of two constituent terms for the zirconium alloy tubes are as follows:

$$k = 1.1 \times 10^7 \exp\left(-\frac{87.0}{RT}\right) \text{ for Zircaloy-2 tube,} \quad (3a)$$

$$k = 6.9 \times 10^7 \exp\left(-\frac{100.0}{RT}\right) \text{ for Zircaloy-4 tube, and} \quad (3b)$$

$$k = 1.5 \times 10^6 \exp\left(-\frac{75.3}{RT}\right) \text{ for ZIRLO}^{\text{TM}} \text{ tube.} \quad (3c)$$

The activation energy is expressed in kJ/mol.

The results show that the activation energy for the hydriding reaction of the ZIRLO™ tube is the lowest

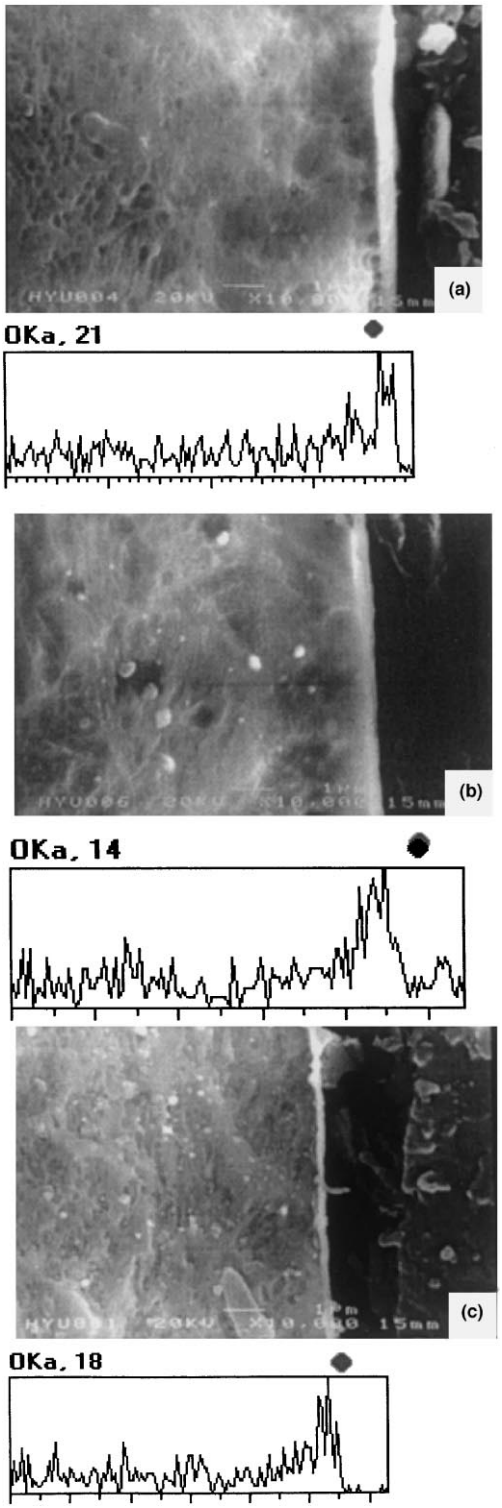

Fig. 4. Oxygen concentration profiles of cross-sectioned hydrided zirconium alloy tubes at 350°C: (a) Zircaloy-2; (b) Zircaloy-4; (c) ZIRLO™.

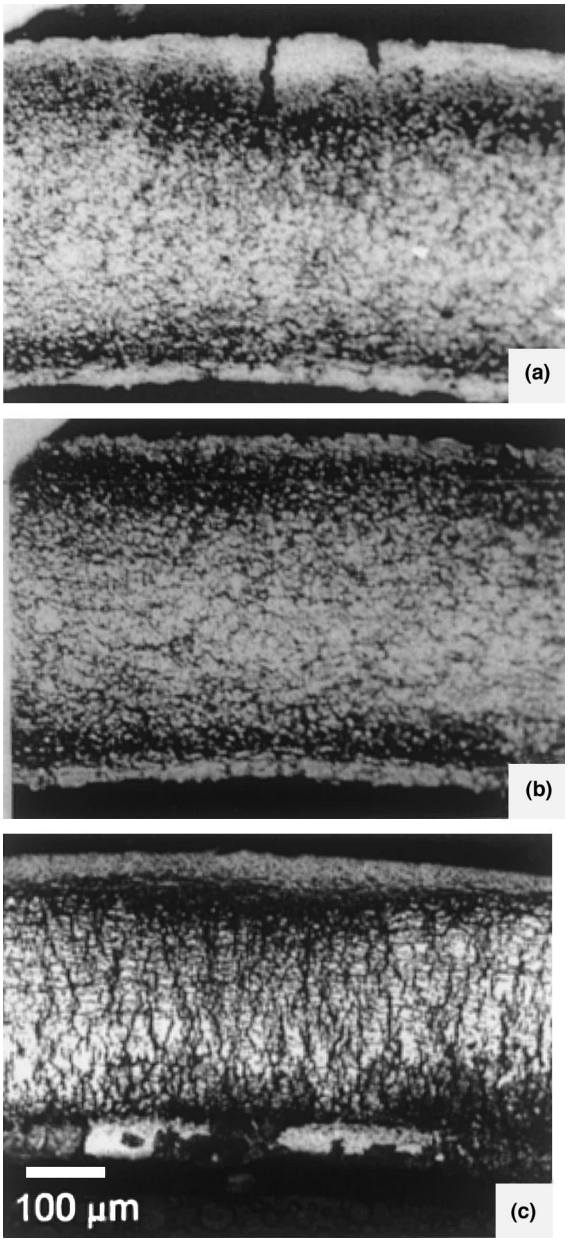

Fig. 5. Micrographs of hydride distribution and orientation at around 5000 ppm: (a) Zircaloy-2; (b) Zircaloy-4; (c) ZIRLO™.

and that for the Zircaloy-4 tube is the highest. The activation energy for Zircaloy-2 is in the middle and found to be 87.0 kJ/mol, a little higher than the previous result of 68.2 kJ/mol [6]. The kinetic rate constants for the three Zircaloy tubes are collected for comparison in Fig. 8.

At temperatures lower than 400°C, a slight deviation from linear kinetics is observed in all specimens (Fig. 6(a)–(c)). It seems to be ascribed to slow diffusion

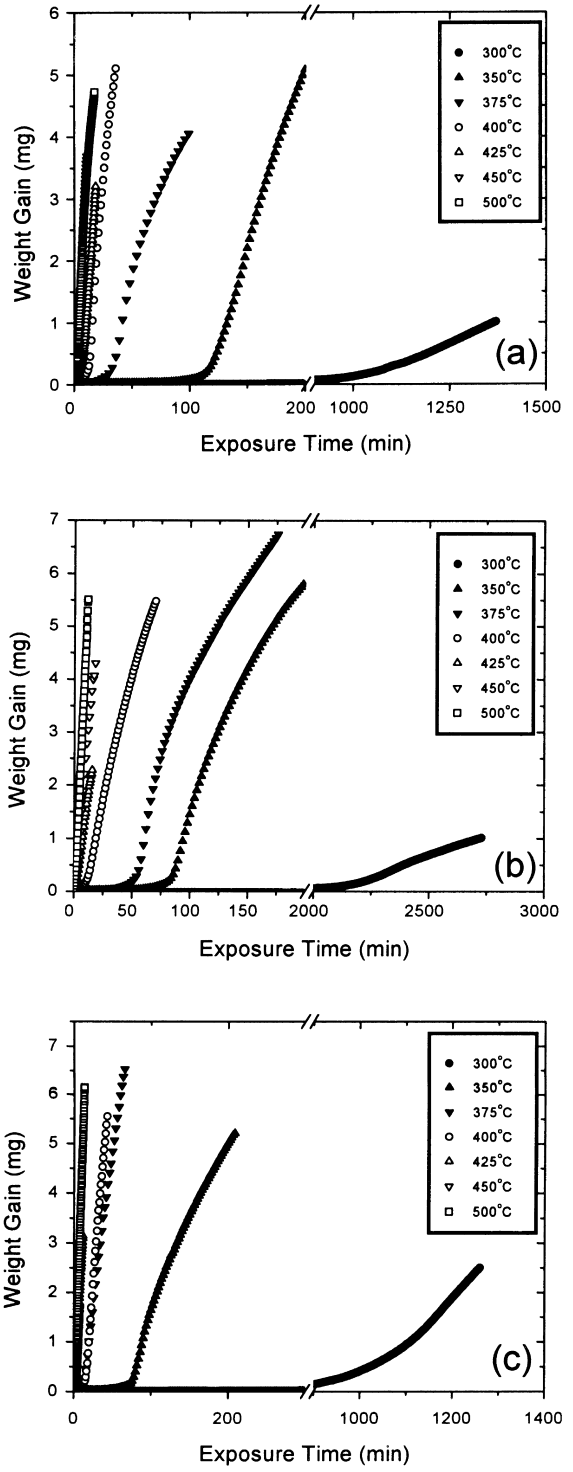

Fig. 6. Weight gain behaviors in the hydrided reaction of zirconium alloy tubes at several temperatures: (a) Zircaloy-2; (b) Zircaloy-4; (c) ZIRLO™.

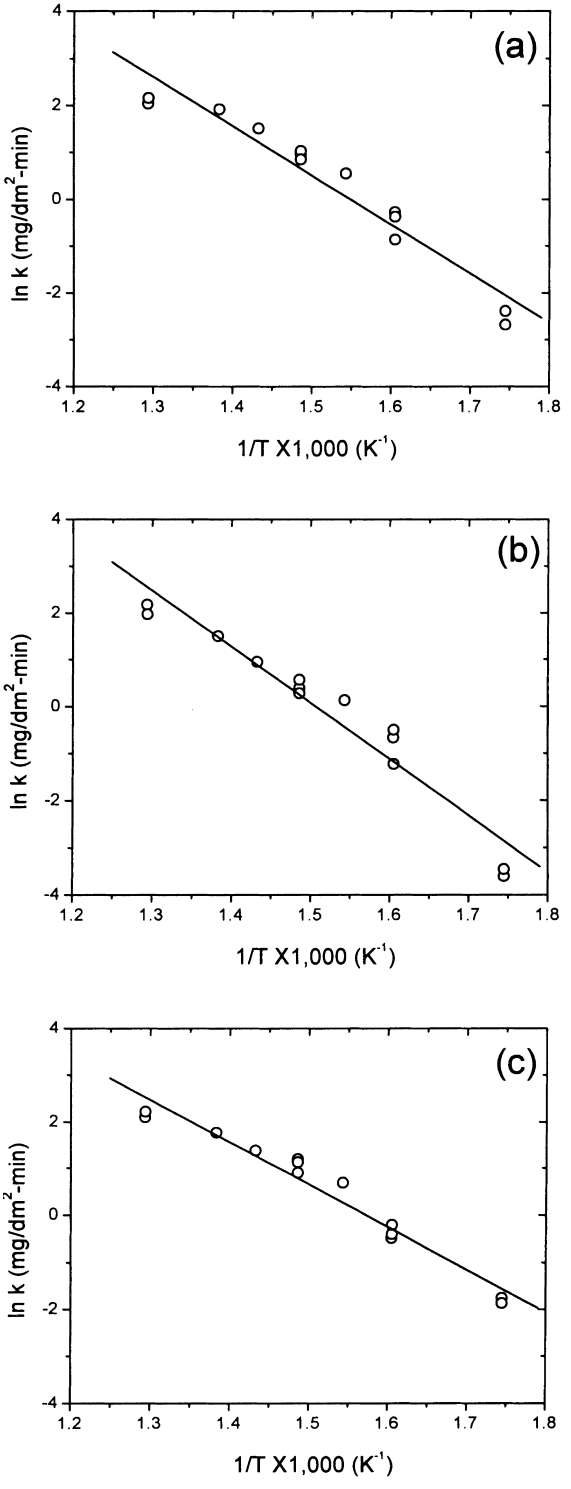

Fig. 7. Arrhenius plots of hydriding reaction rates: (a) Zircaloy-2; (b) Zircaloy-4; (c) ZIRLO™.

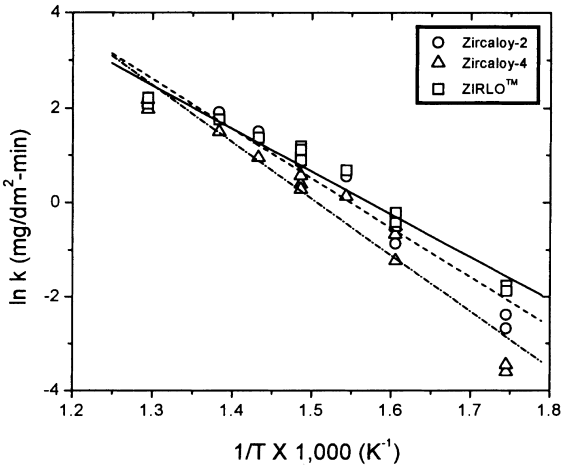

Fig. 8. Comparison of the hydriding reaction rates of Zircaloy-2, Zircaloy-4, and ZIRLO™ tubes.

of hydrogen atoms through hydride layer at the temperatures. It is known that δ-hydride ($ZrH_{1.6}$) layer forms on the surface and grows to be ε-hydride ($ZrH_{1.8}$) layer as hydrogen concentration increases. The diffusion of hydrogen in δ and ε-hydride phase is slower than in α-Zr [10–16], and thus, the slow diffusion may compete with the rate-determining step of surface reaction. However, at high temperatures above 400°C, the diffusion process becomes relatively faster, and therefore, the deviation from the linear rate law disappears.

It has been known that sunburst-type localized massive hydriding occurs only under in-pile conditions with temperature gradient [17] or on the contaminated, especially fluoride-contaminated surface [18]. However, despite no temperature gradient, sunburst-type localized hydriding phenomenon is observed mostly at the inner surfaces of all three zirconium alloy tube specimens with hydrogen content above 1000 ppm. The morphologies for the localized massive hydridings are shown in Fig. 9. Severely hydrided damage of the Zircaloy-2 tube, a form of cracks in the sunburst region and flaked-off hydride chips, is shown in Fig. 9(a). Fig. 9(b) and (c) show the initial stages of the localized hydriding attack of the Zircaloy-4 and ZIRLO™ tubes, respectively. These figures explicitly reveal the importance of surface condition in the massive hydriding damage of zirconium alloy tubes.

4. Conclusions

Kinetic studies on the massive hydriding of commercial Zircaloy-2, Zircaloy-4, and ZIRLO™ tubes are carried out in the temperature range of 300–500°C under atmospheric pressure by in situ measurements with

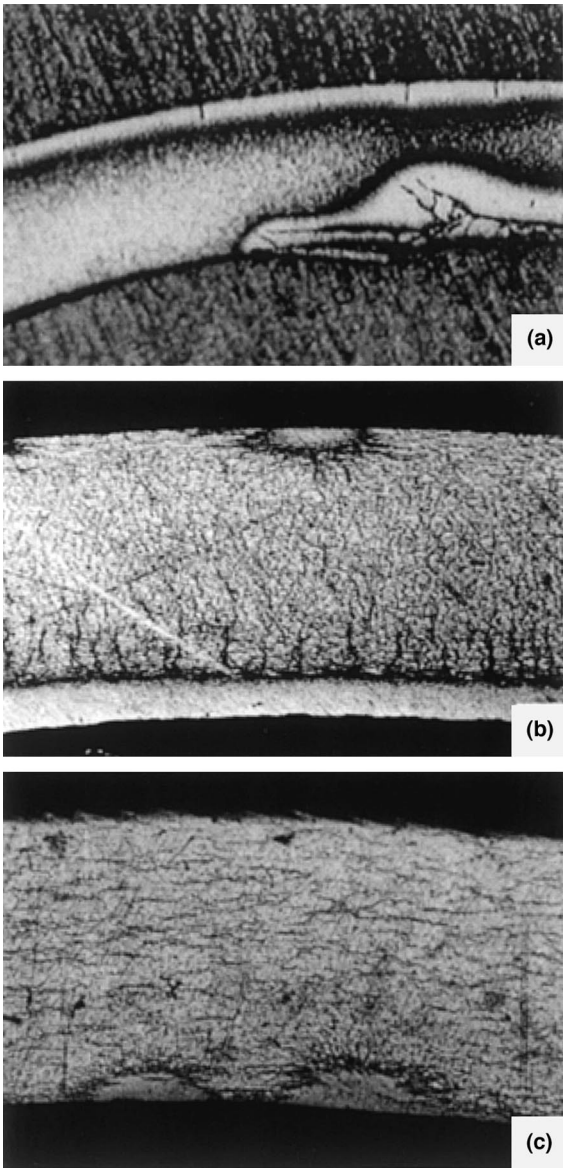

Fig. 9. Micrographs of sunburst-type localized hydriding without temperature gradient: (a) Zircaloy-2 (5500 ppm); (b) Zircaloy-4 (2000 ppm); (c) ZIRLO™ (2,000 ppm).

TGA. From the experimental results, the following conclusions are drawn.

1. The massive hydriding kinetics follow a linear rate law after incubation time caused by thin surface oxide film grown during the prior heating.
2. The reaction rates of Zircaloy-2, Zircaloy-4, and ZIRLO™ tubes derived on the basis of linear kinetics are $1.1 \times 10^7 \exp(-87.0/RT)$, $6.9 \times 10^7 \exp(-100/RT)$, and $1.5 \times 10^6 \exp(-75.3/RT)$ mg/dm^2 min, respectively, where activation energies are in kJ/mol.
3. Slight retardation from the linear kinetics is observed at temperatures lower than 400°C. It is attributed to slower diffusion of hydrogen atoms through surface hydride layer at the low temperatures.
4. Even without temperature gradient, sunburst-type localized massive hydriding can occur even with hydrogen content around 1000 ppm. This demonstrates the importance of surface condition in massive hydriding damage.

Acknowledgements

This paper was supported by the Non-Directed Research Fund, Korea Research Foundation, 1996.

References

[1] J.C. Clayton, ASTM STP 1023, 1989, p. 266.
[2] D.R. Olander, S. Vaknin, EPRI TR-101773 (1993).
[3] R.F. Boyle, T.J. Kisiel, WAPD-BT-10, 1958, p. 31.
[4] E.A. Gulbransen, K.F. Andrew, Metall. Trans. 185 (1949) 515.
[5] J. Belle, B.B. Cleland, M.W. Mallett, J. Electrochem. Soc. 101 (1954) 211.
[6] K. Une, J. Less Common Met. 57 (1978) 93.
[7] S. Naito, J. Chem. Phys. 79 (1983) 3113.
[8] G. Meyer, M. Kobrinsky, J.P. Albriata, J.C. Bolcich, J. Nucl. Mater. 229 (1996) 48.
[9] J. Bloch, I. Jacob, M.H. Mintz, J. Alloys Compounds 191 (1993) 179.
[10] M.W. Mallet, W.H. Albrecht, J. Electrochem. Soc. 104 (1957) 142.
[11] E.A. Gulbransen, K.F. Andrew, J. Electrochem. Soc. 101 (1954) 560.
[12] W.M. Mueller, J.P. Blackledge, G.G. Libowitz, Metal Hydrides, 1968, p. 296.
[13] J.F. Hon, J. Chem. Phys. 36 (1962) 759.
[14] K.R. Doolan, P.P. Narang, J.M. Pope, J. Phys. 10 (1980) 2073.
[15] R. Chang, USAEC Report NAA-SR-5537, 1960.
[16] J.M. Pope, P.P. Narang, K.R. Doolan, Phys. Chem. Solids 42 (1981) 519.
[17] F. Garzarolli, R. von Jan, H. Stehle, Atomic Energy Rev. 17 (1979) 31.
[18] L. Lunde, J. Nucl. Mater. 44 (1972) 241.